Articles

Contribution from the Discipline of Coordination Chemistry and Homogeneous Catalysis, Central Salt and Marine Chemicals Research Institute, Bhavnagar 364002, India

Ruthenium(III) Chloride in Aqueous Solution: Kinetics of the Aquation and Anation Reactions of the Chloro Complexes

M. M. Taqui Khan,* G. Ramachandraiah, and R. S. Shukla

Received March 11, 1988

Kinetics of aquation and anation reactions of $[RuCl_4(H_2O)_2]^-$ (**1**), $[RuCl_3(H_2O)_3]$ (**2**), $[RuCl_2(H_2O)_4]^+$ (**3**), and $[RuCl(H_2O)_5]^{2+}$ (**4**) species were studied spectrophotometrically at 25 °C. The studies reported here include the effect of initial concentration of these species, the hydrogen ion concentration (0.1–1 M), and potassium chloride concentration (0.01–1 M) on aquation and anation rates. Species **1** exists in a protonated form **1a** with a lower aquation rate than **1**. An acid-catalyzed induced stability for **2** and **4** is responsible for their lowered rates of decay with decreasing pH. Probable mechanisms for all the conversion steps are proposed and the corresponding rate constants computed. With the help of the data obtained, it is concluded that species **2** is the stable product in 10 mM ruthenium(III) chloride in 1 M HCl stock solution.

Introduction

In the preceeding paper[1] we have reported the changes in spectral and electrochemical behavior of a millimolar solution of ruthenium(III) chloride in 0.1 M KCl in the pH range 0–2. In these solutions, the chloro species present are $[RuCl_4(H_2O)_2]^-$ (**1**), $[RuCl_3(H_2O)_3]$ (**2**), $[RuCl_2(H_2O)_4]^+$ (**3**), and $[RuCl(H_2O)_5]^{2+}$ (**4**). Each of these species was characterized,[1,2] by assigning individual ligand-to-metal charge-transfer absorption bands and redox potentials. We have also reported the percentage content of each chloro species existing in a freshly prepared millimolar solution of ruthenium(III) chloride. The effect of aging of these solutions on the species distribution was also investigated.

In the present paper, the kinetics of aquation or anation reactions of **1–4** in dilute aqueous solution is investigated at 25 °C in the pH range 0–2 at μ = 0.1 M KCl. The present data are useful in identifying the type of chloro complexes that exist in solution and their behavior in dilute hydrochloric acid under a given set of experimental conditions. The observed rate data are extrapolated to zero pH and the conversion rates for each species in the complicated[3-7] multiion equilibria investigated. From these data were calculated the half-lives for all these catalytically important species.[8-12] The most stable species in 1 M hydrochloric acid was identified, and the probable mechanisms and rate laws were proposed.

Experimental Section

Materials and Methods. The stock solution of ruthenium(III) (20 mM) was prepared in 1 M hydrochloric acid and estimated by the method described earlier.[1] The stock solution was stored in a standard flask of Pyrex glass at 25 °C.

The physicochemical techniques used to measure solution pH and high speed time-drive absorption data were reported[1] earlier.

Kinetic Measurements. In general, a kinetic run consists of measuring absorbance data at 25 °C for each λ_{max} value (Table I) at an interval of 5 min for a total duration of 60 min. The absorption data are then converted into species concentrations by employing molar extinction coefficients and plotted against time to obtain initial rates of aquation, anation, formation, or polymerization depending on the species and its behavior. During these calculations, the decay in concentration of the species, in general, is considered as aquation, anation, or polymerization, while the increase in species concentration with time is considered as its formation from other species. The total ruthenium(III) ion concentration in all these experimental solutions was varied in the range of 1–0.1 mM. The required pH of these solutions was adjusted by employing 1 M HCl or 0.1 M carbonate-free sodium hydroxide[13] solutions. Suitable amounts of 1 M KCl were used to maintain the required ionic strength in solution. Each of the kinetic runs was initiated by mixing thoroughly, made up to a constant volume, an appropriate amount of ruthenium(III) stock solution with a solution containing suitable amounts of KCl, acid/base, and distilled water. The solution mixture was then immediately transferred to the matched cuvet of 10-mm path length, and the kinetics was followed by recording the characteristic absorption spectra of species **1–4** in the range 200–500 nm.

Table I. Characteristic Absorption and Reduction Potential Data for Ruthenium(III) Chloro Complexes

chloro complex	$-E_{1/2}$, V vs Ag/AgCl	λ_{max}, nm (ϵ, M^{-1} cm^{-1})
$[RuCl_4(H_2O)_2]^-$	0.180	269 (37 025)
$[RuCl_3(H_2O)_3]$	0.270	322 (6314)
$[RuCl_2(H_2O)_4]^+$	0.355	376 (6928)
$[RuCl(H_2O)_5]^{2+}$	0.415	456 (32 655)

Results and Discussion

The spectral behavior of a freshly prepared millimolar ruthenium(III) chloride solution (pH 1.0) on heating to different temperatures is shown in Figure 1. A new broad band at 322 nm and a band of low intensity at 377 nm appeared with the simultaneous disappearance of the band at 269 nm, as shown in Figure 1e. The broad band at 322 nm, which is masked[1] in the minima between 269 and 377 nm, is probably due to a mixture of two isomeric forms[4] of **2** in solution. On the basis of the data from the earlier report[1] and present observations, the characteristic charge-transfer (LMCT) bands with the corresponding extinction coefficients and the redox potentials for Ru(III)/Ru(II) couples are summarized in Table I.

(1) Taqui Khan, M. M.; Ramachandraiah, G.; Prakash Rao, A. *Inorg. Chem.* **1986**, *25*, 665.
(2) Taqui Khan, M. M.; Ramachandraiah, G., unpublished work.
(3) Cady, H. H.; Connick, R. E. *J. Am. Chem. Soc.* **1958**, *80*, 2646.
(4) Connick, R. E.; Fine, D. A. *J. Am. Chem. Soc.* **1960**, *82*, 4187; **1961**, *83*, 3414.
(5) Rard, J. A. *Chem. Rev.* **1985**, *85*, 1–39 and ref 404b, 434, 457, 467–69, and 473 therein.
(6) Grube, G.; Fremm, G. *Z. Elektrochem. Angew. Phys. Chem.* **1939**, *45*, 871.
(7) Sclenskaya, V. I.; Kuratashvili, Z. A.; Tikhonov, I. G. *Chem. Abstr.* **1973**, *78*, 164990.
(8) Taqui Khan, M. M.; Siddiqui, M. R. H.; Amjad Hussain.; Moiz, M. A. *Inorg. Chem.* **1986**, *25*, 2765.
(9) Taqui Khan, M. M.; Prakash Rao, A. *J. Mol. Catal.* **1986**, *35*, 48.
(10) Taqui Khan, M. M.; Shukla, R. S. *J. Mol. Catal.* **1986**, *37*, 269; **1987**, *39*, 139.
(11) Taqui Khan, M. M.; Shaukat, A. M.; Bajaj, H. C. *J. Mol. Cat.* **1986**, *37*, 253; **1987**, *39*, 323.; *React. Kinet. Catal. Lett.*, in press. Taqui Khan, M. M.; Prakash Rao, A.; Shukla, R. S., submitted for publication in *J. Mol. Catal.*
(12) Riley, D. P. *J. Chem. Soc., Chem. Commun.* **1983**, 1530.
(13) Schwarzenbach, G.; Biederman, R. *Helv. Chim. Acta* **1948**, *31*, 337.

0020-1669/88/1327-3274$01.50/0

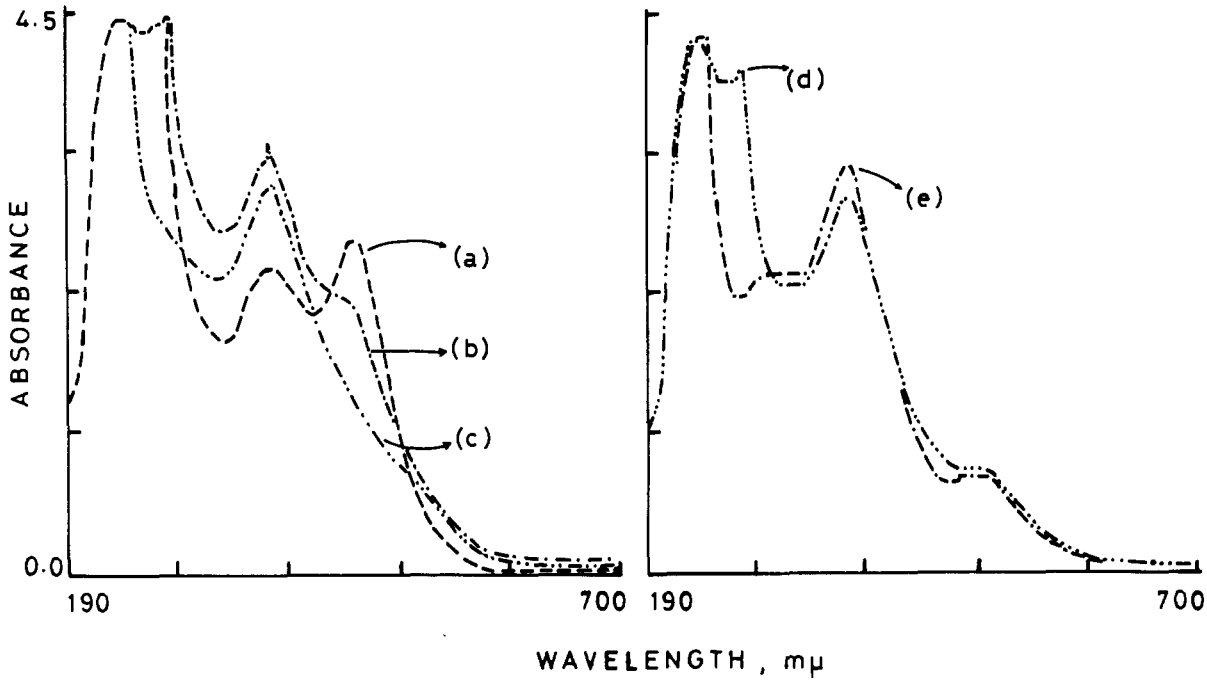

Figure 1. Demonstration of absorption spectral changes in ruthenium(III) chloride (mM) (pH 1.0, μ = 0.1 M (KCl), 25 °C) at different heating conditions: (a) solution before heating; (b) solution after heating to 70 °C; (c) solution b heated to boil; (d) solution c boiled for 10 min; (e) solution d after 24 h.

Kinetics of aquation, anation, or polymerization reactions of **1**–**4** are thus followed by observing the changes in their characteristic band intensities at 269, 322, 377, and 456 nm, respectively. These reactions, in general are represented by the interdependent equilibria (2)–(5), where the forward reaction represents aquation and the reverse reaction, anation.

$$\underset{\mathbf{1}}{[RuCl_4(H_2O)_2]^-} + H^+ \overset{K}{\rightleftharpoons} \underset{\mathbf{1a}}{H[RuCl_4(H_2O)_2]} \quad (1)$$

$$\underset{\mathbf{1a}}{H[RuCl_4(H_2O)_2]} + H_2O \overset{k_1}{\underset{k_{-1}}{\rightleftharpoons}} \underset{\mathbf{2}}{[RuCl_3(H_2O)_3]} + Cl^- + H^+ \quad (2)$$

$$\underset{\mathbf{1}}{[RuCl_4(H_2O)_2]^-} + H_2O \overset{k_1'}{\underset{k_{-1}'}{\rightleftharpoons}} \underset{\mathbf{2}}{[RuCl_3(H_2O)_3]} + Cl^- \quad (3)$$

$$\underset{\mathbf{2}}{[RuCl_3(H_2O)_3]} + H_2O \overset{k_2}{\underset{k_{-2}}{\rightleftharpoons}} \underset{\mathbf{3}}{[RuCl_2(H_2O)_4]^+} + Cl^- \quad (4)$$

$$\downarrow k_{p1}$$

polymeric species

$$\underset{\mathbf{3}}{[RuCl_2(H_2O)_4]^+} + H_2O \overset{k_3}{\underset{k_{-3}}{\rightleftharpoons}} \underset{\mathbf{4}}{[RuCl(H_2O)_5]^{2+}} + Cl^- \quad (5)$$

Since the complex $[RuCl_5(H_2O)]^{2-}$ exists in the presence of a large concentration of HCl, >6 M, its presence is considered negligible in the pH range investigated. The formation of $[Ru(H_2O)_6]^{3+}$ is likewise negligible in the said pH range. Accordingly, the aquation reactions of the penta- and monochloro complexes are negligible in the present investigation, and they have not been taken into consideration. The influence of KCl in the range 0.01–1 M over the equilibria (2)–(5) was checked at a constant pH of 1.67. The studies indicate that none of the above equilibria were affected much. Thus KCl effects were considered as secondary; i.e., it merely contributes to ionic strength of the medium. The various rate constants so computed for reactions 2–5 at the said pH are listed in Table II. Some of the species **1**–**4** exist as different geometrical isomers.[4] It is difficult to assess their amounts in solution. Therefore, each of the rate constants reported here may be considered as the mean of the contribution of the possible isomers to the rate.

Table II. Observed and Calculated[a] First-Order Rate Constants for the Conversion of Ruthenium(III) Chloro Complexes at μ = 0.1 M (KCl) and t = 25 °C

first-order rate const	pH	10^4k, s^{-1}	first-order rate const	pH	10^4k, s^{-1}
k_1'	1.67	1.30	k_{-2}	1.67	0.29[a]
k_{-1}'	1.67	0.43[a]	k_3	1.67	0.05[a]
k_1	0.80	0.12	k_{-3}	1.67	0.18
k_{-1}	0.80	0.03[a]	k_{p1}	1.67	0.37
k_2	1.67	0.34			

[a] Calculated by using equilibrium constants reported in ref 1 and rate constants observed in present studies.

Kinetics of Aquation of $[RuCl_4(H_2O)_2]^-$ (1). The aquation reaction of **1** was studied by following the decrease in the intensity of the characteristic absorption band at 269 nm at various initial concentrations of species **1** in solution. The concentration of **1** in these studies was varied from 0.038 to 0.126 mM with the pH at 1.67, μ at 0.1 M (KCl), and temperature at 25°. The initial rate $-d[\mathbf{1}]/dt$ was calculated by considering the least-squares curve fitting for the initial 60 min of the plot of concentrations of **1** versus time (Figure 2A). The log–log plot of initial rates, $-d[\mathbf{1}]/dt$, versus initial concentrations of **1** is depicted in Figure 2B. It shows a linear first-order dependence on initial concentration of **1**. The first-order rate constant k_1' obtained from the slope of the least-squares fit of the plot $-d[\mathbf{1}]/dt$ versus [**1**] is 1.3×10^{-4} s^{-1}.

It is evident from the log–log plot (Figure 2B) that the decay rates at higher (>0.126 mM) and lower (< 0.038 mM) concentrations of **1** deviate from the average first-order plot. In dilute solutions, however, the deviation can be attributed to the weakening of hydrogen bonding[1] between the identical species of **1**.

The effect of hydrogen ion concentration in the pH range 0.27–2.05 on rate of aquation of **1** was studied by keeping the total ruthenium(III) concentration at 0.4 mM in 0.1 M KCl. The results are listed in Table IIIA. The corrected pH versus log $(-d[\mathbf{1}]/dt)$ profile is shown in Figure 3. It is evident from this plot that the rate of aquation of **1** follows an inverse first-order dependence on hydrogen ion concentration in the pH range 0.7–1.8 and is independent on either side of these pH limits.

The inverted S-type pH–logarithmic rate profile (Figure 3) is explained on the basis of the assumption that complex **1** exists in the protonated and normal forms **1a** and **1**, respectively (eq

Table III. Kinetic Data at t = 25 °C and μ = 0.1 M (KCl) for (A) the pH Dependence on $-d[1]/dt$ ($[Ru(III)]_T$ = 0.4 mM), (B) the Concentration Dependence of **2** on $-d[2]/dt$ (pH 1.67), and (C) the Concentration Dependence of **3** on $d[3]/dt$ and k_p (pH 1.67)

A		B		C		
pH	$10^7(-d[1]/dt)$, M min^{-1}	$10^4[2]$, M	$10^7(-d[2]/dt)$, M min^{-1}	$10^4[3]$, M	$10^7(d[3]/dt)$, M min^{-1}	10^7k_p, M min^{-1}
0.27	0.31	0.79	1.32	0.84	0.62	1.10
0.79	0.43	1.79	2.46	1.84	0.65	1.86
0.83	0.67	1.84	3.59	1.93	0.81	2.70
1.29	1.55	2.10	4.18	2.20	1.00	3.41
1.67	4.83	2.41	4.72	2.51	3.47	4.15
1.69	4.36	3.30	5.63	3.41	8.21	4.98
2.05	4.47	4.06	8.21	4.38	9.29	10.66

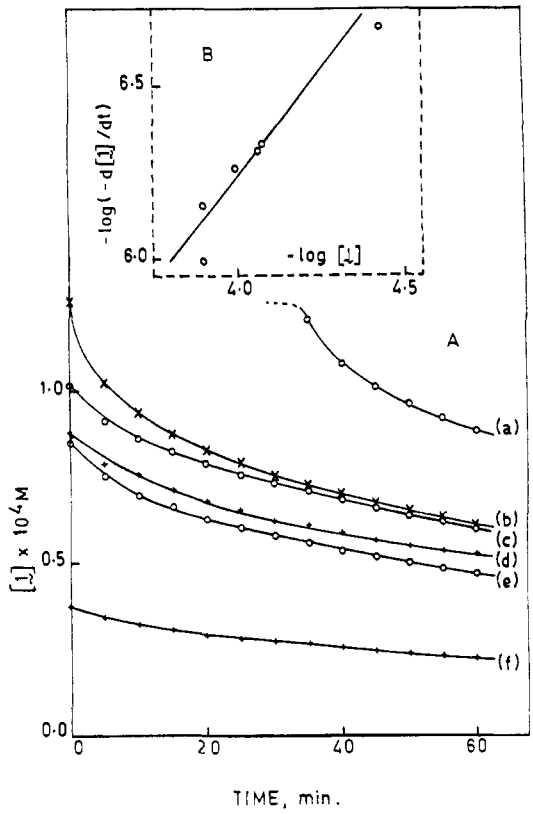

Figure 2. (A) Effect of initial concentration of $[RuCl_4(H_2O)_2]^-$ on rate of its aquation (pH 1.67; [KCl] = 0.1 M, 25 °C). 10^4 $[[RuCl_4(H_2O)_2]^-]$: (a) 1.264 M; (b) 1.264 M; (c) 1.016 M; (d) 0.866 M; (e) 0.845 M; (f) 0.376 M. (B) Plot of $-\log(-d[1]/dt)$ vs $-\log[1]$ (25 °C, μ = 0.1 M (KCl), pH 1.67).

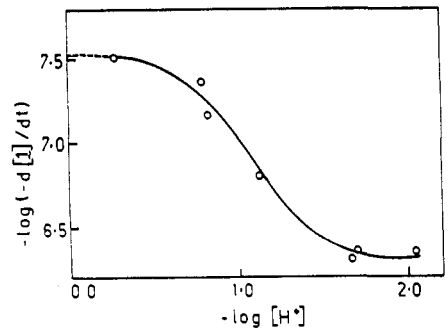

Figure 3. Plot of the logarithm of the rate of aquation of $[RuCl_4(H_2O)_2]^-$ vs pH (25 °C, μ = 0.1 M (KCl), $[Ru(III)]_T$ = 0.4 mM).

1) whose aquation rates are different in solution. The protonated complex **1a** is stable at lower pH (<0.7) and is totally converted to the normal form **1** at higher pH (>1.8) with an equilibrium between **1** and **1a** in the pH range 0.7–1.8. Thus, the midpoint of the inflection in the log–log plot (Figure 3) at pH 1.1, where these two chloro complexes are 50% interconverted, is approximately considered to be the acid dissociation constant ($K_a = 1/K$) of $H[RuCl_4(H_2O)_2]$ (**1a**). The minimum dissociation rate $-d[1]/dt$ ($\sim 3.2 \times 10^{-8}$ M min^{-1}) can be attributed to the protonated complex **1a** (reaction 2), while the maximum rate $-d[1]/dt$ ($\sim 4.7 \times 10^{-7}$ M min^{-1}) is assigned to the normal complex **1** (reaction 3). Therefore, the net rate of aquation of **1** can be written as

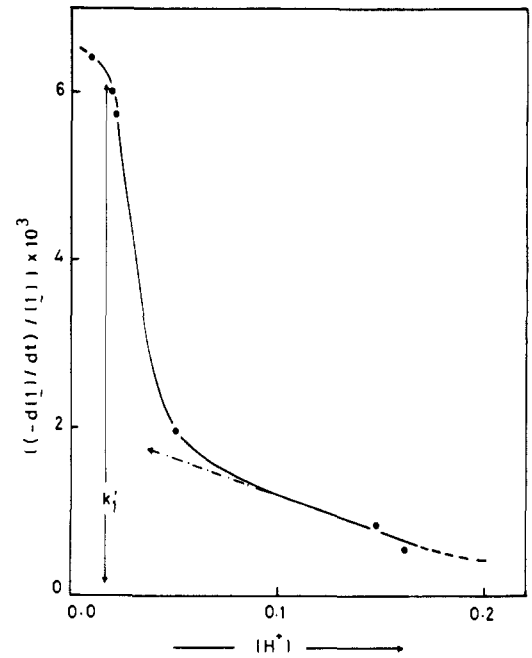

Figure 4. Plot of $(-d[1]/dt)/[1]$ vs $[H^+]$ (25 °C, μ = 0.1 M (KCl), $[Ru(III)]_T$ = 0.4 mM).

$$-d[1]/dt = (k_1K[H^+] + k_1')[1] \quad (6)$$

The plot of $(-d[1]/dt)/[1]$ versus $[H^+]$ is shown in Figure 4. It is evident from this plot that eq 6 is valid only within the limits of hydrogen ion concentrations 0.02–0.16 M (pH 1.7–0.8), beyond which the rate becomes independent of $[H^+]$. At lower hydrogen ion concentrations, the term $k_1K[H^+] < k_1'$; hence, the rate $-d[1]/dt$ is governed by reaction 3. Under this approximation, the rate $(-d[1]/dt)/[1]$ gives the rate constant k_1'. At a value of $[H^+] = 1.6 \times 10^{-2}$ M, the value of k_1' is 1.04×10^{-4} s^{-1}. However, at hydrogen ion concentrations between 0.04 and 0.17 M where $k_1K[H^+] \approx k_1'$, the rate $-d[1]/dt$ is considered as the net contribution of reactions 2 and 3. From K_a ($10^{-1.1}$) and the slope of the tangent drawn at the points of $[H^+]$, 0.09–0.17 M, the rate constant k_1 was calculated as 1.16×10^{-5} s^{-1}. The rate constants k_{-1} and k_1' were calculated with the help of equilibrium data[1] reported earlier.

Kinetics of Aquation and Anation of $[RuCl_3(H_2O)_3]$ (2). The kinetics of aquation and anation of **2** was followed by observing the increase (formation) and the decrease (aquation or anation) in intensity of the band at 322 nm at regular intervals of time as a function of its concentration, pH, and KCl concentration. Table IIIB presents the rate of decay in concentration of **2** as a function of its initial concentrations at pH 1.67 and μ = 0.1 M (KCl). Since the formation of **1** was not seen in these experimental conditions, the decay in concentration of **2** is considered for its aquation (reaction 4). The data in Table IIIB show a first-order dependence

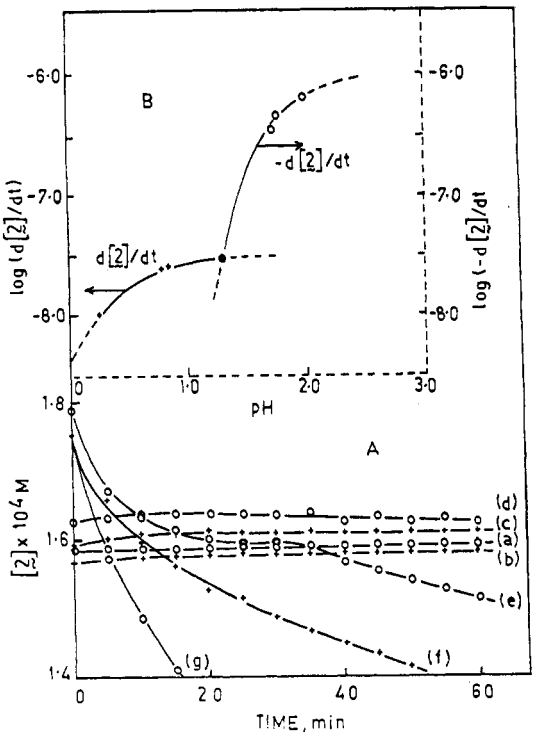

Figure 5. (A) Effect of the acidity on the rates of aquation and formation of $[RuCl_3(H_2O)_3]$ (25 °C, μ = 0.1 M (KCl), $[Ru(III)]_T$ = 0.4 mM. pH: (a) 0.27; (b) 0.79; (c) 0.83; (d) 1.29; (e) 1.67; (f) 1.69; (g) 2.05. (B) Plots of log (d[**2**]/dt) and log (−d[**2**]/dt) vs pH (25 °C, μ = 0.1 M (KCl, $[Ru(III)]_T$ = 0.4 mM).

of rate of aquation (−d[**2**]/dt) of **2** on its initial concentrations. The first-order rate constant, k_2, determined from the plot of rate (−d[**1**]/dt) versus initial concentration of **2** is 3.40×10^{-5} s^{-1}.

The effect of hydrogen ion concentration on the rate of aquation of **2** was observed in the pH range 0.27–2.05. During these studies, the total metal ion concentration $[Ru(III)]_T$ and KCl concentrations were maintained constant at 0.4 mM and 0.1 M, respectively. The experimental results are plotted as the changes in concentration of **2** as a function of time; the curves are depicted in Figure 5A. The figure shows that the formation of **2** is facilitated at lower pH (<1.3) and aquation at higher pH (>1.3). The rates of formation, d[**2**]/dt, were thus evaluated from the points of ascending concentrations, while the aquation rates were evaluated from the points of descending concentrations of the plots of Figure 5A. The log–log plots of initial rates d[**2**]/dt and −d[**2**]/dt versus pH are shown in Figure 5B. It is observed from Figure 5B that the aquation rate, −d[**2**]/dt, tends to level off (6.6×10^{-7} M min^{-1}) at pH ~2 and decreases drastically below pH 1.7. The rate of formation, d[**2**]/dt, on the other hand is independent of pH in the range 0.7–1.3 and decreases as pH decreases below 0.7. The rate of formation of **2**, d[**2**]/dt, can be calculated by the rate expression (7), which is the algebraic sum of the rates of aquation of **1** or **1a** (reactions 2 and 3) and anation of **3** into **2** (reaction 4).

$$d[\mathbf{2}]/dt = (k_1K[H^+] + k_1')[\mathbf{1}] + k_{-2}[\mathbf{3}] \quad (7)$$

A steady-state concentration of **2** may be assumed at pH 1.3 (Figure 5B), where the rate of formation of **2**, d[**2**]/dt, equals the rate of aquation, −d[**2**]/dt. Since the rate of aquation, −d[**2**]/dt, has a first-order dependence in [**2**] and inverse dependence in $[H^+]$, it can be written as

$$-d[\mathbf{2}]/dt = k_2[\mathbf{2}]/[H^+] \quad (8)$$

The rate of formation (5.9×10^{-7} M min^{-1}) calculated from eq 7 was found to be comparable with the aquation rate (4.1×10^{-7} M min^{-1}) calculated from eq 8 by using the observed data at pH 1.3. This verified the validity of the rate expressions (7) and (8) and supports the proposed steps. The rate constant k_{-2} is calculated as discussed in the latter part of this section.

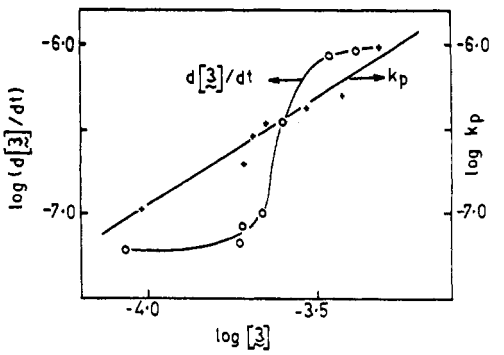

Figure 6. Plots of the logarithms of rate of formation, d[**3**]/dt, and rate of polymerization, k_p, vs the logarithm of the initial concentration of **3** (pH 1.67, [KCl] = 0.1 M, 25 °C).

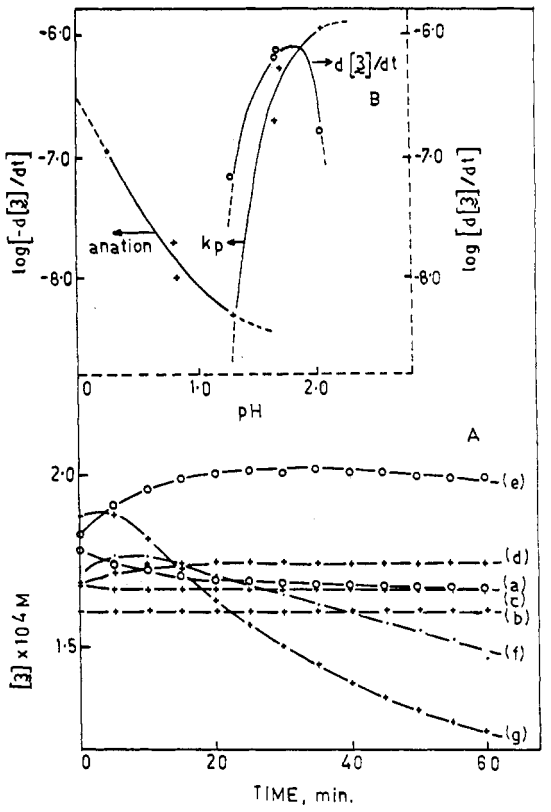

Figure 7. (A) Effect of acidity on the rates of formation and polymerization of $[RuCl_2(H_2O)_4]^+$ (25 °C, μ = 0.1 M (KCl), $[Ru(III)]_T$ = 0.4 mM; pH (a)–(g) as described in the caption of Figure 5). (B) Plots of log (d[**3**]/dt), log (−d[**3**]/dt), and k_p vs pH (25 °C, μ = 0.1 M (KCl), $[Ru(III)]_T$ = 0.4 mM).

Kinetics of Aquation and Anation of $[RuCl_2(H_2O)_4]^+$ (3). The changes in the concentrations of complex **3** with time were followed by observing absorption band at 377 nm under a given set of experimental conditions. The results at different initial concentrations of **3** at pH 1.67 and 0.1 M KCl indicate initially an increase in [**3**] followed by its decay. According to the earlier findings,[1] the decay of **3** is accounted for by its polymerization. The initial rates of formation of **3** (d[**3**]/dt) were thus measured by considering the points of the ascending concentrations and the rates of polymerization, k_p, measured from the points of the descending concentrations. The rate data are presented in Table IIIC. The logarithmic plots of initial rates, d[**3**]/dt, versus initial concentrations of **3** and k_p as a function of **3** are shown in Figure 6. The rate k_p shows a linear first-order dependence on [**3**], while d[**3**]/dt has no dependence on its concentration except a break in the curve in the concentration range of **3** of $(2.0–3.2) \times 10^{-4}$ M. The reason for this break is the domination of k_p over the rates of formation, d[**3**]/dt, at lower concentrations of **3** (<3.0×10^{-4} M) and vice versa at higher concentrations. The first-order

Table IV. Kinetic Data at t = 25 °C and μ = 0.1 M (KCl) for (A) the Concentration Dependence of [**4**] (pH 1.67) and (B) the pH Dependence on $-d[\mathbf{4}]/dt$ ($[Ru(III)]_T$ = 0.4 mM)

A		B	
10^4[**4**], M	$10^7(-d[\mathbf{4}]/dt)$, M min^{-1}	pH	$10^7(-d[\mathbf{4}]/dt)$, M min^{-1}
1.20	7.35	0.79	0.15
0.98	5.62	0.83	0.29
0.72	4.94	1.29	0.97
0.65	3.48	1.67	3.24
0.57	3.25	1.69	3.38
0.53	3.24	2.05	3.39
0.24	1.43		

polymerization rate constant k_{p1} obtained from the plot of k_p versus [**3**] is 3.72 × 10^{-5} s^{-1}.

Figure 7A represents the effect of hydrogen ion concentration on the rates k_p and d[**3**]/dt of the dichloro complex **3**. The data show that the formation of **3** in terms of the increase in concentration of **3** appeared at higher pH (>1.0). Figure 7A also shows the decay of the concentration of **3**, due to its polymerization, decreased from pH 2.05 to pH 1.30. However, the decay of the concentration of **3** started to increase over its rates of polymerization or formation as pH decreased further from 1.3, because of its predominant anation (the back-reaction in eq 4). The rates of anation of **3** ($-d[\mathbf{3}]/dt$) at pH 0.27–1.3 were determined from the points of descending concentration of **3**. The log–log plots of k_p versus pH, d[**3**]/dt versus pH, and $-d[\mathbf{3}]/dt$ versus pH are given in Figure 7B. It is evident from Figure 7B that the formation of **3** is maximum at pH 1.8 and decreases drastically on either side of this pH value. Also, the k_p profile indicates that species **3** has a greater tendency toward polymerization at pH >2.0. The decrease in d[**3**]/dt at pH <1.8 is mostly accounted for by the induced stability in **1** and **2**, while at pH >2.0, it is accounted for by its predominant polymerization over its formation. The lowered rates of polymerization, k_p, of **3** are considered to be due to its induced stability during acid-catalyzed addition[14-16] of chloride ions.

The rate expression for the formation of **3** from species **2** and **4** is given by

$$d[\mathbf{3}]/dt = k_2[\mathbf{2}] + k_{-3}[\mathbf{4}] \quad (9)$$

The rate of formation, d[**3**]/dt, thus calculated from eq 9 by substituting the rate data for conversion of **2** and **4** to **3** at pH 1.67 is 1.03 × 10^{-6} M min^{-1}. Similarly, the rate of decrease in concentration of **3**, $-d[\mathbf{3}]/dt$, is also calculated with the help of eq 10 and found to be 1.00 × 10^{-6} M min^{-1} at pH 1.67.

$$-d[\mathbf{3}]/dt = k_{p1}[\mathbf{3}] + k_{-2}[\mathbf{3}] \quad (10)$$

Table V. Rate Data and Half-Lives for the Conversion of Ruthenium(III) Chloro Complexes in 1 M HCl to the Stable Species $[RuCl_3(H_2O)_3]$ at 25 °C

species	rate × 10^8,[a] M min^{-1}	$t_{1/2}$, days
$[RuCl_4(H_2O)_2]^-$	2.985	1.3
$[RuCl_3(H_2O)_3]$	43.7	
$[RuCl_2(H_2O)_4]^+$	33.11	0.24
$[RuCl(H_2O)_5]^{2+}$	0.11	22.5

[a] Anation or aquation obtained by extrapolation to pH 0.

Kinetics of Anation of $[RuCl(H_2O)_5]^{2+}$ (4). The decay in the concentration of **4** with time was measured by monitoring the absorption band at 465 nm as a function of initial concentration, pH, and KCl concentration. Under these experimental conditions, the decay of **4** is due to its conversion to **3** or to polymeric products as reported earlier.[1] Here we have considered only the decay of **4** mainly by its anation. The observed rate data, $-d[\mathbf{4}]/dt$, at various initial concentrations and pH are given in Table IV. The rate, $-d[\mathbf{4}]/dt$, has a linear first-order dependence on the initial concentrations of **4**. The rates are independent of H^+ ions at pH >1.7 and dependent below pH 1.7. It is possible that the monochloro complex is stabilized at lower pH by protonation from HCl, which leads to the acid-catalyzed formation[1,14-16] of various chloro complexes. The first-order rate constant k_{-3} for the anation of **4** (reaction 5) calculated from the plot of $-d[\mathbf{4}]/dt$ versus initial concentrations of **4** is 1.82 × 10^{-5} s^{-1}.

Conclusion

It may be concluded from the rate data in Table II that the forward reactions of (3) and (4) and the backward reaction of (5) are more favorable in dilute solutions than their corresponding reverse reactions. Because of this reason, species **1**, **2**, and **4** revert to **3** in dilute solutions at pH >1.0. The rates $-d[\mathbf{1a}]/dt$, d[**2**]/dt, $-d[\mathbf{3}]/dt$, and $-d[\mathbf{4}]/dt$ obtained by extrapolation to pH 0 are given in Table V. It is obvious from these data that the aquation of **1** to **2** and anation of **4** to **3** to give species **2** in 1 M HCl stocks of ruthenium chloride are very favorable. It means that species **2** is the most stable chloro complex of ruthenium(III) if the stock solutions of ruthenium chloride possessed with complicated multiion equilibria are allowed to age. Hence, the present investigation quantitatively supports the long time for ruthenium(III) chloride to reach thermodynamic equilibrium as predicted[3-7] earlier.

(14) McBryde, W. A.; Yeo, J. H. *Anal. Chem.* **1948**, *20*, 1094.
(15) Sandell, E. B. *Colorimetric Determination of Trace Metals*, 2nd ed.; Interscience: New York, 1950; p 527.
(16) Wehner, P.; Hindman, J. C. *J. Phys. Chem.* **1952**, *56*, 10.